Patch Recordings from the Electrocytes of *Electrophorus electricus*

Na Currents and P_{Na}/P_K Variability

SCOTT SHENKEL and FREDERICK J. SIGWORTH

From the Department of Cellular and Molecular Physiology, Yale University School of Medicine, New Haven, Connecticut 06510

ABSTRACT Sodium currents were recorded in cell-attached and inside-out patches from the innervated membrane of *Electrophorus* electrocytes. Electrocytes from Sachs and main electric organs were prepared as described by Pasquale et al. (1986. *J. Membr. Biol.* 93:195.). Maximal currents in the Sachs organ, measured with 1–2-μm diameter patch pipettes and at room temperature, were in the range of 20 to 300 pA (27 patches) and were obtained near +10 mV. This range of current corresponds to ~70 to 1,300 channels in a patch. Maximal current in main organ cells also occurred near +10 mV and were in the range of 100 to 400 pA. Delayed K current was observed in a few patches. The inactivation phase of the currents during maintained depolarizations appears to be a single-exponential relaxation. The time constant decreases from 1 ms near −55 mV to a minimum of 0.3 ms near 0 mV, and then gradually increases with stronger depolarization. The mean currents are half inactivated near −90 mV with an apparent voltage dependence of *e*-fold per 6 mV. No apparent differences were observed in the decay time course or steady-state inactivation of the currents in the same patch before and after excision. From ensemble fluctuation analysis the peak open probability was found to be ~0.5 at +25 mV and increased only gradually with larger depolarizations. The single channel conductances were ~20 pS with 200 mM Na outside and 200 mM K inside, and 40 pS in 400 mM solutions. Reversal potentials in the 200 Na//200 K solutions ranged from +51 to +94 mV in multichannel patches, corresponding to selectivity ratios P_{Na}/P_K from 8 to 43. Large differences in reversal potentials were seen even among patches from the same cell. Several controls rule out obvious sources of error in the reversal potential measurements. It is concluded that there is heterogeneity in the selectivity properties of the Na channels.

INTRODUCTION

The first voltage-gated Na channel to be purified biochemically (Agnew et al., 1978; Miller et al., 1983) and to be cloned and sequenced (Noda et al., 1984) is that present

Address reprint requests to Dr. Scott Shenkel, Department of Cellular and Molecular Physiology, Yale University School of Medicine, 333 Cedar Street, P.O. Box 3333, New Haven, CT 06510-8026.

J. GEN. PHYSIOL. © The Rockefeller University Press · 0022-1295/91/05/1013/29 $2.00
Volume 97 May 1991 1013–1041

in the electrocytes of the main electric organ of the electric eel *Electrophorus electricus*. However, little has been reported concerning the biophysical properties of the channel in its native environment. This paper presents a characterization of the Na channel currents in membrane patches of eel electrocytes. Of special interest are some features of gating and ion selectivity that appear to differ from those of other sodium channels that have been studied.

The innervated membrane of an *Electrophorus* electrocyte is electrically excitable, having an estimated Na channel density of $\sim 500\ \mu m^{-2}$ (Keynes and Martins-Ferreira, 1953; Levinson, 1975). The inward Na current that underlies the generation of the electrocyte action potential is tetrodotoxin sensitive (Nakamura et al. 1965; Grundfest, 1966). Termination of the action potential occurs mainly as a result of Na channel inactivation (reviewed in Grundfest, 1966). Earlier studies did not report the presence of a delayed K current, but inward-rectifying K channels that close upon small depolarizations from rest are present (Nakamura et al., 1965).

The properties of *Electrophorus* Na channels have been studied after reconstitution into artificial membranes (Rosenberg et al., 1984*a*, *b*; Recio-Pinto et al., 1987; Shenkel et al., 1989; Correa et al., 1990). Studies of Na currents in the native tissue have been hampered by the difficulty of voltage-clamping this preparation (Nakamura et al., 1965; Lester, 1978). The alternative approach used here is to patch-clamp small membrane areas (Hamill et al., 1981). Recently, Pasquale et al. (1986) succeeded in recording currents through single nicotinic acetylcholine receptor channels from electrocytes after a dissection procedure involving enzymatic and mechanical treatment. A similar procedure was used in this study to allow recording of currents in electrocytes from the Sachs and main electric organs. A preliminary account of this work has previously appeared (Shenkel, 1989).

METHODS

Preparation and Electrocyte Dissection

The electric organ of *Electrophorus* consists of the main organ, the organ of Sachs, and Hunter's organ, which together occupy most of the posterior three-quarters of the animal. The electrocytes are arrayed in rows and columns in these organs and are flattened in the anterior-posterior direction. Only the innervated, posterior membrane is excitable (Keynes and Martins-Ferriera, 1953). The electrocytes from each organ have similar morphological and electrical properties (Keynes and Martins-Ferreira, 1953; Luft, 1957; for review see Bennett, 1971). Most of the experiments described here were performed on the electrocytes from the organ of Sachs, but recordings from main organ electrocytes were made for comparison.

Electrophorus electricus, 30–100 cm in length, were obtained from World Wide Scientific (Orlando, FL). The dissection procedure used here is similar to that described in Pasquale et al. (1986). A portion of the organ with surrounding skin was removed by a transverse cut 8–10 cm from the end of the tail. Transverse slices two to three cell layers thick were made from this section and placed in extracellular solution (mM: 200 NaCl, 3 $CaCl_2$, 1.5 $MgCl_2$, 5 Hepes(NaOH), pH 7.2) containing 1 mg/ml collagenase type IV from *Clostridium histolyticum* and 1 mg/ml hyaluronidase type-IV-S (Sigma), Chemical Co., St. Louis, MO, for 5–10 min at room temperature (22–24°C). We found that enzyme treatment was not always necessary for removing connective tissue from the electrocytes of the smaller eels; no apparent differences in the time course and voltage dependence of activation and inactivation were observed among

currents recorded from electrocytes with and without enzyme treatment. Patches from cells dissected in the absence of enzyme treatment are indicated in the figure and table legends.

After several rinses, a slice was pinned to the Sylgard[R] (Dow Corning Corp., Midland, MI) bottom of a plexiglass chamber with its innervated membrane facing up, and it was viewed under a dissecting microscope at a magnification of 40. The relatively thick collagenous sheet containing spinal nerves and blood vessels, which blankets the innervated face, was removed with forceps. A much thinner sheet, which occasionally adhered tightly to the cell surface (Pasquale et al., 1986), was also removed. Before each experiment the chamber was rinsed repeatedly and filled with an "intracellular" solution (mM): 200 KCl, 2 $MgCl_2$, 1 EGTA, 5 Hepes(KOH), pH 7.2 (200 K solution). In some experiments a similar solution was used, but with 400 μM KCl. In other experiments, 200 NaCl or 20 NaCl + 327 sucrose was substituted for KCl in the bath. The intracellular Na solutions were titrated with NaOH. In the text, "outside" and "inside" refer to the extracellular and intracellular faces of the patch membrane, respectively. Description of solutions (in millimolar units) given in the text will be written according to the convention outside solution//inside solution. Experiments could be performed for 2 d following the dissection. All macroscopic currents were measured on the day of the dissection. By the second day, after storing the tissue overnight in an extracellular solution at 4°C, the channel activity in a patch was reduced to ~ 1/100 of that of freshly dissected cells and it was during this time that single-channel recordings were made. The time course and voltage dependence of activation and inactivation were similar for macroscopic and single-channel currents measured on day 1 and day 2, respectively (see Results). All experiments were performed at room temperature, 22–24°C.

Current Measurement

Patch pipettes were fabricated (Hamill et al., 1981) from KIMAX-51 glass capillaries (Kimble Products, Vineland, NJ) and filled with extracellular solution (mM): 200 NaCl, 3 $CaCl_2$, 1.5 $MgCl_2$, 5 Hepes(NaOH), pH 7.2 (200 Na solution). In some experiments a similar solution was used, but with 400 NaCl. The pipette resistances were ~3 MΩ in the 200 Na solution. The apparent seal resistance R_{seal}, which represents the parallel combination of leakage resistance through the seal and the resistance of the patch membrane itself, was determined from the difference in currents at the end of a prepulse and the end of a test pulse for each patch. Values of R_{seal} were typically tens of gigohms (Table I). The major obstacle in obtaining gigohm seals on this preparation was the relatively large amount of connective tissue covering the innervated membrane. In ~50% of the slices in which the connective tissue was easily removed from individual cells, the fraction of successful seals was ~75%. The success rate was lower on those cells to which the connective tissue adhered more tightly. In general, connective tissue was more easily removed from main organ cells, however they were more difficult to dissect because of their small size. The lifetime of the patches listed in Table I ranged from 1 to 68 min, with an average of 14 min. Most recordings were made in the "inside-out" patch configuration, obtained by simply withdrawing the pipette from the cell after establishing a seal. In ~10% of the excisions this led to unusual current recordings, which probably reflected resealing of the membrane to form a closed vesicle. In about half of these cases the currents appeared normal after passing the pipette tip through the air-solution interface. Some cell-attached measurements were made in order to compare currents before and after excision; in those experiments the K-containing bath solution was assumed to zero the cells' resting potential.

The current signal from an EPC-7 patch-clamp amplifier (List Medical, Darmstadt, FRG) was filtered with a low-pass Bessel filter at 3–10 kHz and sampled at five times the bandwidth by a computer-based data acquisition system (Affolter and Sigworth, 1988). The filtering probably distorted the rapid activation phase of some current records, since even at 10 kHz the filter risetime is ~30 μs. However, we expect that the voltage control of the patch membrane was

adequate: the stimulus risetime on the EPC-7 was set to 2 μs, and because of the low capacitance of the patch membrane and the speed of the current-to-voltage converter, all other time constants in the voltage control of the membrane are expected to be < 1 μs. Potentials were corrected for a measured diffusion potential of −5 mV in those experiments performed with 200 Na//200 K solutions. The diffusion potential was measured in the following way: With an open pipette in the bath, the electrode potential difference was zeroed with 200 mM Na

TABLE I

Na Current Parameters in Inside-Out Patches from Sachs Organ Electrocytes with 200 Na//200 K Solutions

File	Cell*	E_r	P_{Na}/P_K	I_{max}	τ_h	R_{seal}
		mV		*pA*	*ms*	*GΩ*
3319a.1a	1	60	11	42	0.40	40
3319b.2a	2	74	19	25	0.37	16
4219a.1a	3	63	13	63	0.34	8
4219a.2a	3	87	32	61	0.32	20
5169a.1a	4	59	11	85	0.22	22
5169a.2a	4	51	8	68	0.23	24
5169b.1a	5	81	26	126	0.24	21
6149a.2b	6	52	8	112	0.45	3
6149a.4c	7	84	29	32	0.32	11
6149a.5c	7	72	18	53	0.33	23
6149a.6c	7	70	16	19	0.36	10
6149b.1a	8	77	22	49	0.48	21
6149b.2a	8	73	18	70‡	—§	16
8159a.1a	9	92	40	174	0.29	54
8159c.1b	10	83	28	223	0.28	9
8159c.2b	10	84	29	320	0.29	8
8159c.3b	10	82	27	291	0.26	63
8179a.n1	11	68	15	76	0.29	33
8179b.1a	12	77	22	262	0.30	27
8179c.1b	13	83	28	174	0.29	35
8179c.2b	13	80	24	325	0.28	16
8179c.3b	13	90	37	80‡	—	8
10199a.1b	15	51	8	126	0.28	29
10199b.1c	16	75	20	261	0.26	35
10199b.1a	17	90	36	133	0.29	11
10249a.1a	18	87	33	107	0.28	12
11159a.1a	19	88	34	205	0.25	27
Mean ± SD		75 ± 14			0.31 ± 0.06	

*Cells 11, 12, and 13 were dissected without using enzyme treatment.

‡Estimated from partial peak current-voltage relation. Reversal potentials (E_r) were obtained as fits to Eq. 1. τ_h Values were obtained from depolarizations to +5 mV by visual fits to the declining phase of Na current as in Fig. 3.

§Current not measured at +5 mV.

solution in the pipette and 200 mM Na solution in the bath. The diffusion potential was taken as the potential difference after switching to 200 K solution in the bath. For data analysis, capacitive current cancellation and leak subtraction were performed by using P/4 pulses (Benzanilla and Armstrong, 1977) applied from a holding potential of −125 mV. The experiments shown are from recordings made on inside-out patches from Sachs organ electrocytes, except where indicated.

RESULTS

Fig. 1 shows a family of macroscopic currents and the peak current-voltage relation from an inside-out patch in 200 Na//200 K. Each trace represents the average of 10 consecutive sweeps after P/4 subtraction. A current of 5 pA was detected near −55 mV and a maximal inward current of 262 pA flowed at +15 mV. In 27 patches from 18 cells the maximal currents were in the range of 19 to 325 pA and the mean potential for maximal current was +9.8 ± 4.9 mV (SD). The range of peak current probably reflects variations in patch area and channel density.

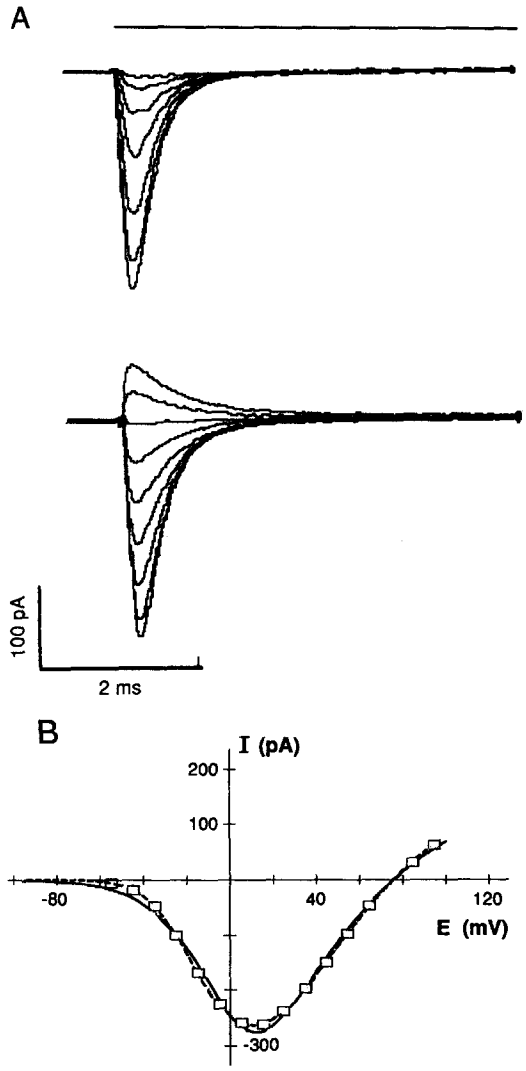

FIGURE 1. (*A*) Currents recorded from an inside-out patch in 200 Na//200 K solutions after P/4 leak subtraction. Inward currents are shown as downward deflections. Currents were elicited by step depolarizations (duration indicated by horizontal bar) to −55 to +5 mV (*top*) and +15 to +95 mV (*bottom*) in 10-mV increments. Pulses were applied at 1-s intervals after a 20-ms hyperpolarizing prepulse to −125 mV from a holding potential of −95 mV. Averages of 10 traces are shown. Filter 5 kHz. Patch currents are from a cell dissected without enzyme treatment. Data file: 8179b.1a. (*B*) Peak current–voltage relation for the currents shown in *A*. The solid curve is a least-squares fit according to Eq. 1 (see text for parameters). The dotted curve is a least-squares fit of the product of the GHK equation and the function

$$\frac{1}{1 + \exp(-z_{a1}F[E - E_{a1}]/RT) + \exp(-z_{a2}F[E - E_{a2}]/RT)}$$

with parameters: $E_{a1} = -15$ mV, $z_{a1} = 3.5$, $E_{a2} = +7.6$, $z_{a2} = 1.3$, $P_{Na}/P_K = 21$, $P_{Na} = 3.5 \times 10^{-5}$ cm/s. The expression above is of the form of the open probability function for a "closed-closed-open" channel-gating scheme. It provides a better fit than the Boltzmann component of Eq. 1 to the steep initial rise of the current in the peak current-voltage relations.

The solid curve in Fig. 1 *B* is a least-square fit to the product of the Goldman-Hodgkin-Katz (GHK) current equation (Goldman, 1943; Hodgkin and Katz, 1949) and a Boltzmann function,

$$I = \frac{P_{Na} EF^2 ((P_K/P_{Na})[K]_i - [Na]_o \exp(-EF/RT))}{RT(1 - \exp[-EF/RT])\{1 + \exp[-z_a F(E - E_a)/RT]\}} \quad (1)$$

where I is the current, P_{Na} is the Na permeability, E is the membrane potential, z_a is the valence of the apparent gating charge, E_a is the midpoint voltage of activation, and $[Na]_o$ and $[K]_i$ are the external and internal concentrations of Na and K, respectively. R, T, and F have their usual meanings. The curve was drawn according to the following parameters: $E_a = +4.4$ mV, $z_a = 1.8$, $P_{Na}/P_K = 21.8$, and $P_{Na} = 3.4 \times 10^{-5}$ cm/s. A better fit in the voltage range of -60 to -20 mV could be obtained by including an additional exponential term in the denominator of Eq. 1 as indicated by the dotted curve (see Fig. 1 legend). However, since the additional term had little influence on the function near the reversal potential, we used fits to the simpler Eq. 1 to determine reversal potentials (and, equivalently, permeability ratios) for the patches listed in Tables I and II.

Delayed Outward Current

A delayed outward current of 1–2 pA was detected in two of the 27 patches listed in Table I. When measured at the end of a 5-ms depolarization of -5 mV, the size of the outward current was only 2.4% and 0.9% of the peak inward current in these patches. Larger outward currents were observed in a few subsequent experiments; Fig. 2 *A* shows a family of current traces from one of these. The current rises with a delay, which decreases with stronger depolarization. Outward current was first detected near -40 mV and a maximal current of ~ 50 pA was recorded within the voltage range $+35$ to $+105$ mV (Fig. 2 *B*). Outward single channel currents (Fig. 2 *C*) have amplitudes that increase with depolarization in the voltage range of -35 to -5 mV, and saturate at ~ 1.7 pA for larger depolarizations. The outward current thus appears to arise from a low density of delayed-rectifying potassium channels.

Na Current Inactivation

The declining phase of the electrocyte Na current appears to be a single-exponential relaxation (Fig. 3 *A*). In some patches the currents decayed to a nonzero level at strong depolarized potentials. In the voltage range of -55 to near 0 mV the inactivation time constant τ_h declines; it then gradually increases with further depolarization. This voltage dependence of τ_h is unaffected by patch excision (Fig. 3 *B*). In 25 inside-out patches from 18 cells the mean value of τ_h at $+5$ mV was 0.31 ± 0.06 ms (SD; Table I). A similar value of 0.30 ± 0.12 (SD, three cells) was obtained in inside-out patches from main organ electrocytes.

Steady-state Na channel fast inactivation was investigated using a two-pulse protocol (Hodgkin and Huxley, 1952). The peak current I_t during a depolarizing test pulse was measured following conditioning prepulses of varying potential E_p and 20-ms duration from a holding potential of either -85 or -95 mV. The 20-ms prepulse length was chosen to be long enough to reach a steady level of inactivation.

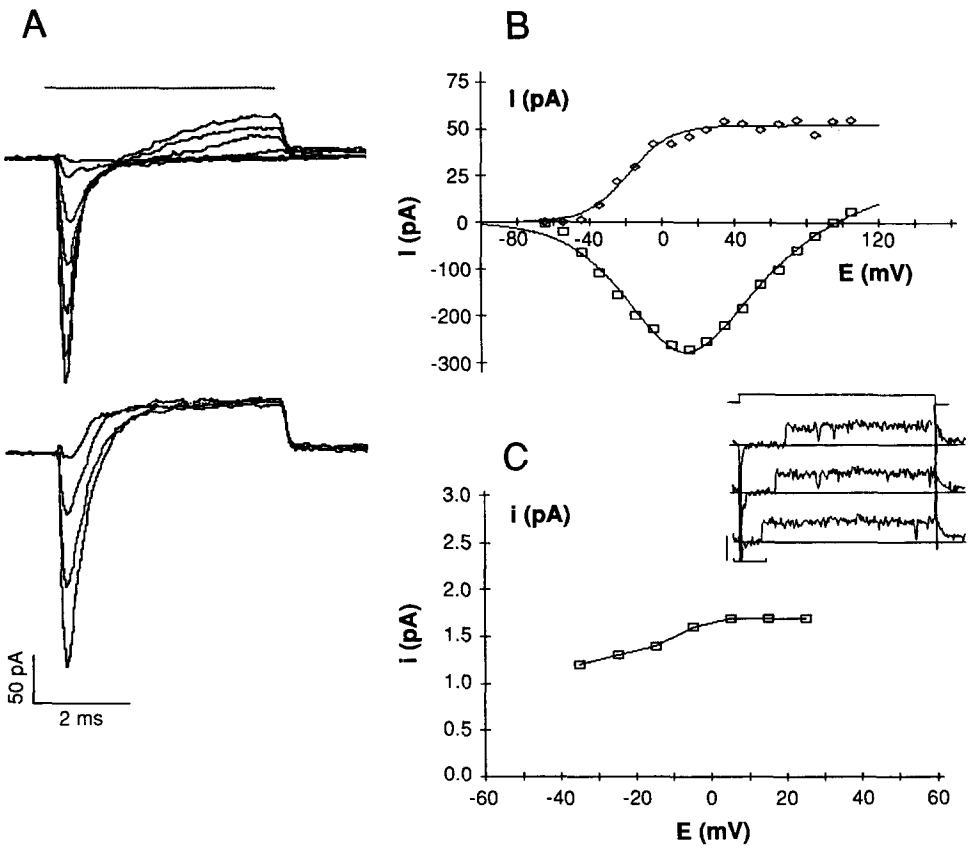

FIGURE 2. Delayed outward currents in 200 Na//200 K solutions. (*A*) Current traces from a patch with particularly large outward currents, shown for depolarizations to −65, −45, −25, and −5 mV (*top*) and +35, +55, +75, and +95 mV (*bottom*). Steps were applied at 1-s intervals for 5 ms (*top bar*) after a hyperpolarizing prepulse to −125 mV from a holding potential of −95 mV. File: 10179A.1a. (*B*) Peak inward (□) and outward (◇) current-voltage relations from the same patch. Note the different scale for inward currents, which were fitted by Eq. 1 with the parameters $E_{1/2}$ = 6.1 mV, z_a = 1.4, P_{Na}/P_K = 47 and P_{Na} = 8.1 × 10^{-6} cm/s (*solid curve*). The peak outward currents I were fitted according to:

$$I = \frac{I_0}{1 + \exp(-zF(E - E_{1/2})/RT)}$$

where the maximal current I_0 = 52 pA, the apparent gating charge valence z = 2.2, and the midpoint voltage $E_{1/2}$ = −19 mV. (*C*) Single-channel current-voltage relation for late outward currents recorded in an inside-out patch from a main organ electrocyte. The pipette contained 400 nM tetrodotoxin to block most of the Na channels. (*Inset*) Three representative single-channel current traces recorded during a 30-ms step depolarization to +5 mV (indicated at top) from a holding potential of −95 mV. Openings are shown as upward deflections from the baseline. Scale bars are 2 pA and 2 ms. Filter 2 kHz. Capacitive current artifacts are present at the start and end of the pulses. File: 12169B.sia.

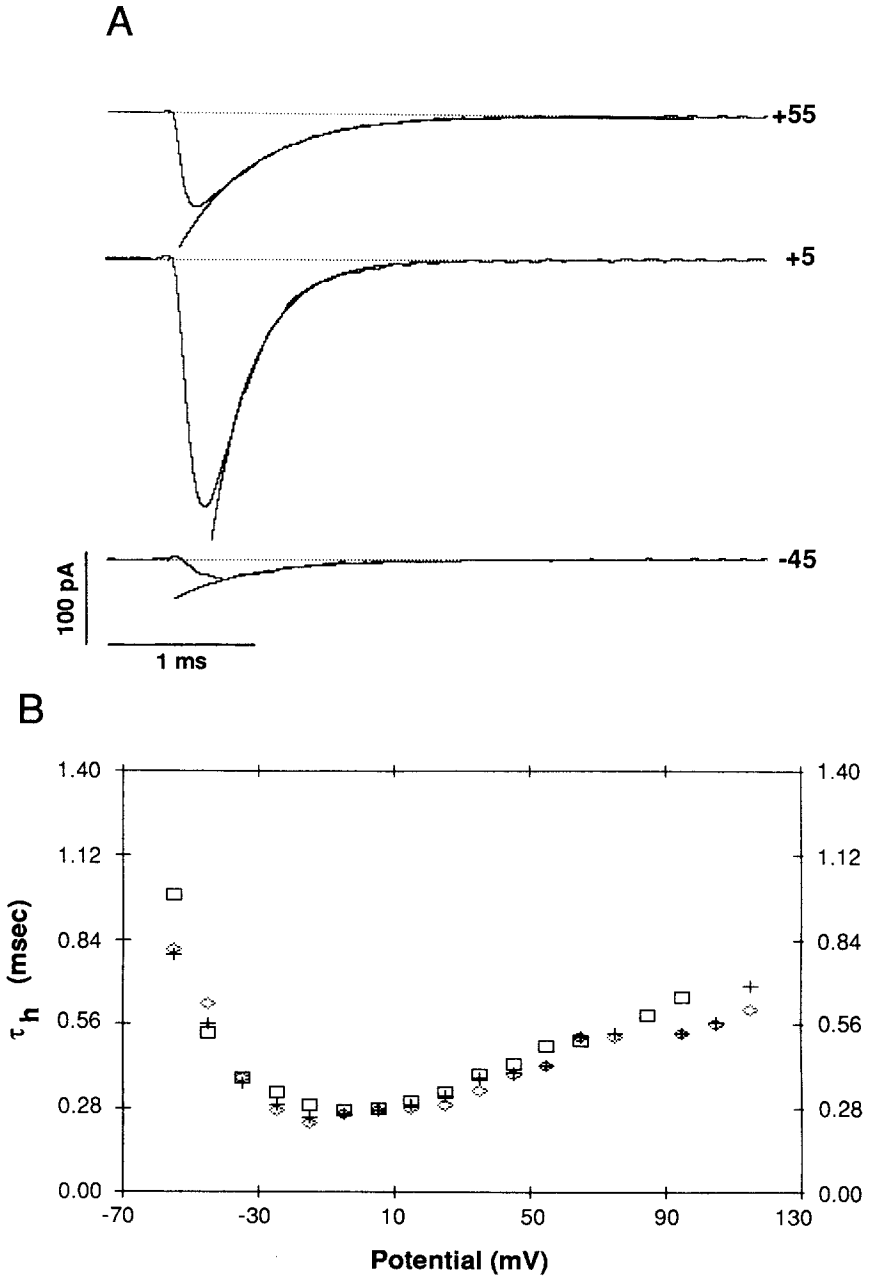

FIGURE 3. Inactivation time constants. (*A*) The inactivation phase of currents fitted with single-exponential relaxations at three different depolarizations. Currents are from the same patch as in Fig. 1. The curves were fit visually with time constants of 0.50 ms (−45 mV), 0.29 ms (+5 mV), and 0.49 ms (+55 mV). (*B*) Voltage dependence of the time constants. (□) Same patch as in Fig. 1; (◇ and +), cell-attached and inside-out recordings from another patch. (+) These data were obtained 20 min after patch excision. Files: (□) 8179b.1a, (◇) 11159a.1a and (+) 11159ao.1a.

Maximal test-current I_{max} was typically obtained with $E_p = -125$ mV. With increasingly positive prepulses, the ratio I_t/I_{max} declined, as illustrated in Fig. 4. The solid curves are least-squares fits to a Boltzmann function,

$$\frac{I_t}{I_{max}} = \frac{1}{1 + \exp(z_h F(E_p - E_h)/RT)} \quad (2)$$

In 11 inside-out patches from nine cells the fitted inactivation midpoint voltage E_h was -93 ± 5 mV and the apparent valence $z_h = 3.9 \pm 0.3$. With an electrocyte resting potential of -90 mV (Bennett, 1971) and these average inactivation parameters,

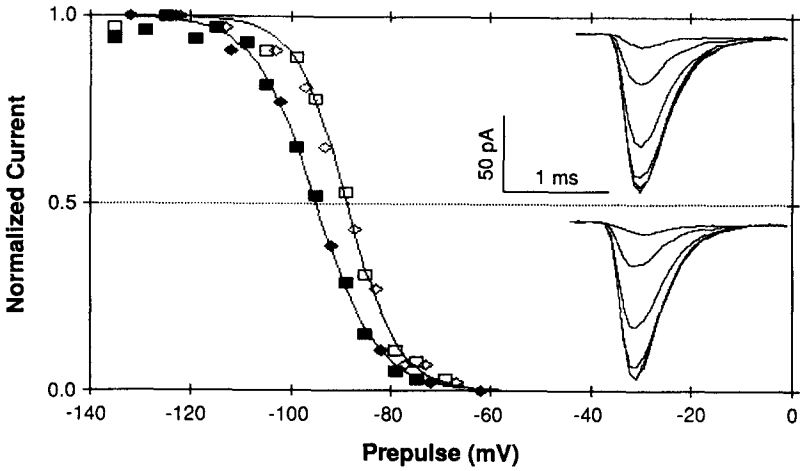

FIGURE 4. Steady-state inactivation of Na current measured with 20-ms prepulses to given potentials. Peak currents during a test pulse to -5 mV were normalized to those at $E_p = -125$ mV. Filled and open symbols correspond to currents in two representative patches, recorded before (*squares*) and after (*diamonds*) patch excision. The steady-state inactivation parameters were determined from a least-squares fit of Eq. 2; the curves show the fits to the cell-attached data. The parameters are: (■): $E_h = -95$ mV, $z_h = 4.1$, (◆): $E_h = -95$ mV, $z_h = 4.0$, and (□): $E_h = -89$ mV, $z_h = 4.9$; (◇): $E_h = -91$ mV, $z_h = 4.3$. (*Inset*) Inward currents from the patch indicated by open symbols obtained with $E_p = -125$ to -75 mV in 10 mV steps, shown before (*top*) and after (*bottom*) patch excision. The test potential was -5 mV. Files: (■) 11159a.1a, (◆) 11159ao.1a, (□) 6149bo.2a, (◇) 6149b.2a.

~60% of the Na channels would be inactivated. Slightly higher values of E_h were obtained in recordings from main organ electrocytes (Table II).

No changes in the steady-state inactivation parameters were observed between cell-attached and inside-out patches. Table II compared these parameters. A direct comparison can be made in the cases of Sachs electrocytes 8 and 19 and main electrocytes 1 and 7, where data were obtained from the same patches. Fig. 4 shows steady-state inactivation curves from two different cells before (*squares*) and after (*diamonds*) excisions of the patches.

The Na current showed some slow inactivation, but was little affected by holding potentials negative to -85 mV. Slow inactivation was investigated in a cell-attached

TABLE II

Steady-State Inactivation Parameters and Reversal Potentials (E_r) in Cell-Attached and Inside-Out Patches from Sachs and Main Organ Electrocytes

File	Cell	E_h	z_h	E_r
A. Sachs organ, cell-attached				
		mV		*mV*
06149bo.2a	8	−89	4.9	73
10199ao.1a	14	−87	4.5	63
11159ao.1a	19	−95	4.1	87
11159ao.2a	20	−90	4.8	100
01100ao.1a	21	−93	5.0	70
Mean ± SD		−91 ± 5	4.7 ± 0.3	79 ± 15
B. Sachs organ, inside-out				
3319a.1a	1	−93	4.0	60
5169a.2a	4	−103	3.3	51
5169b.1a	5	−96	3.7	81
6149b.1a	8	−89	4.1	77
6149b.2a	8	−91	4.3	73
8159c.1b	10	−91	3.9	83
8159c.3b	10	−89	3.9	82
8179b.1a	12*	−95	4.1	77
10199a.1c	16	−87	4.2	51
10249a.1a	18	−91	3.7	87
11159a.1a	19	−95	4.0	88
Mean ± SD		−93 ± 5	3.9 ± 0.3	74 ± 13
C. Main organ, cell-attached				
11219ao.1a	1	−95	3.3	ND
12149ao.1a	1	−95	4.5	90
12149ao.2a	1	−97	4.4	69
12149ao.1c	3	−92	4.8	99
12149bo.1a	4	−95	3.4	70
12149bo.1c	6	−100	3.6	65
Mean ± SD		−96 ± 3	4.0 ± 0.6	79 ± 15
D. Main organ, inside-out				
11219a.1a	1	−97	3.3	ND
12149a.1b	2	−100	4.1	94
12149b.1b	5	−100	4.3	63
12149b.2c	6	−100	4.0	61
Mean ± SD		−99 ± 1	3.9 ± 0.4	73 ± 19

E_h and z_h were estimated from least-squares fits to Eq. 2 as in Fig 4. Reversal potentials are from fits to Eq. 1.
*Cell 12 was dissected in the absence of enzyme treatment.

patch in which the peak current was measured during test pulses to +5 mV preceded by 20-ms prepulses to −125 mV. The relative peak currents measured after 2 min at holding potentials of −125, −95, −85, and −55 mV were 1.0, 0.95, 0.90, and 0.61, respectively.

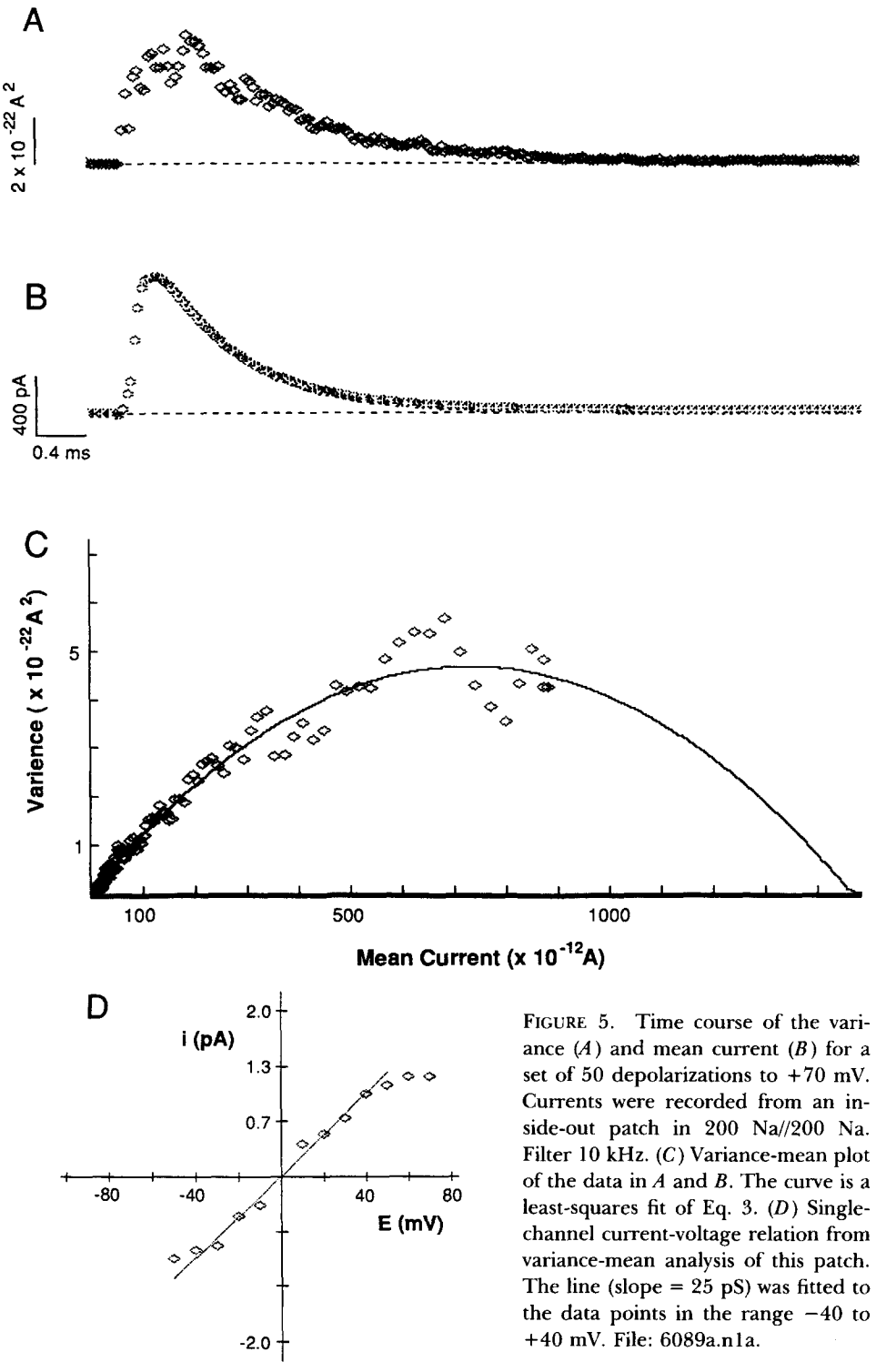

FIGURE 5. Time course of the variance (*A*) and mean current (*B*) for a set of 50 depolarizations to +70 mV. Currents were recorded from an inside-out patch in 200 Na//200 Na. Filter 10 kHz. (*C*) Variance-mean plot of the data in *A* and *B*. The curve is a least-squares fit of Eq. 3. (*D*) Single-channel current-voltage relation from variance-mean analysis of this patch. The line (slope = 25 pS) was fitted to the data points in the range −40 to +40 mV. File: 6089a.n1a.

Fluctuation Analysis

We used ensemble fluctuation analysis (Sigworth, 1980) to obtain estimates for the number of channels in a patch and the single-channel current amplitudes. Depolarizing pulses were applied at 1-s intervals; the holding potential was −95 mV, and 20-ms prepulses to −125 mV were used to remove inactivation. From sets of ~50 consecutive current records at 10 kHz bandwidth, mean and variance time courses were calculated. The background variance was taken to be the average variance during the prepulse; it was subtracted from the variance time course. Fig. 5 *A* shows the mean current $I(t)$ and variance $\sigma^2(t)$ for depolarizations to +70 mV in 200 Na//200 Na solution.

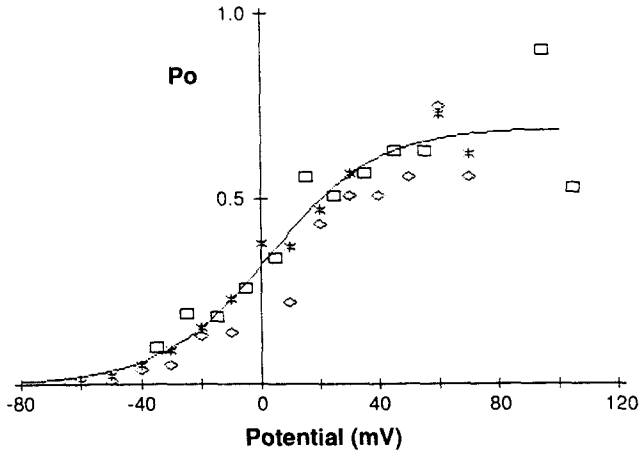

FIGURE 6. Voltage dependence of peak open probability from inside-out patches in: (□) 200 Na//200 K, (+) 100 Na//100 K, and (◇) 200 Na//200 Na (same experiment as in Fig. 5). The solid curve is a least-squares fit of the Boltzmann function

$$P_0 = \frac{P_{max}}{1 + \exp(-z_a F(E - E_a)/RT)}$$

to the data points (□). Here P_{max} is the maximum peak open probability. The fitted parameters were: E_a = +2.9 mV, z_a = 1.4, and P_{max} = 0.69. Files: (□) 8179a.n1a, (+) 5049a.n1b, (◇) 6089a.n1a.

A plot of the variance against the mean current for the data in Figs. 5, *A* and *B* is shown in part *C*. The curve is a least-squares fit to the equation

$$\sigma^2(t) = iI(t) - \frac{I^2(t)}{N} \tag{3}$$

where i is the single channel current amplitude and N is the number of channels. In this fit N was determined to be 1,300 and i = 1.2 pA. The single channel current-voltage relation obtained from variance-mean analysis of this patch (Fig. 5 *D*) shows a conductance of 25 pS.

The peak open probability P_0 was calculated from $P_0 = I_{peak}/Ni$, where N and i were

obtained from curve fitting of Eq. 3 to the variance-mean plots. The peak open probability in three different patches is plotted as a function of voltage in Fig. 6. The values of N were 340, 300, and 1,300, while P_0 values at +25 mV were 0.50, 0.51, and 0.51, respectively. Assuming a reproducible peak open probability at +25 mV, we estimated N to range from 70 to 1,350 in the 27 patches of Table I.

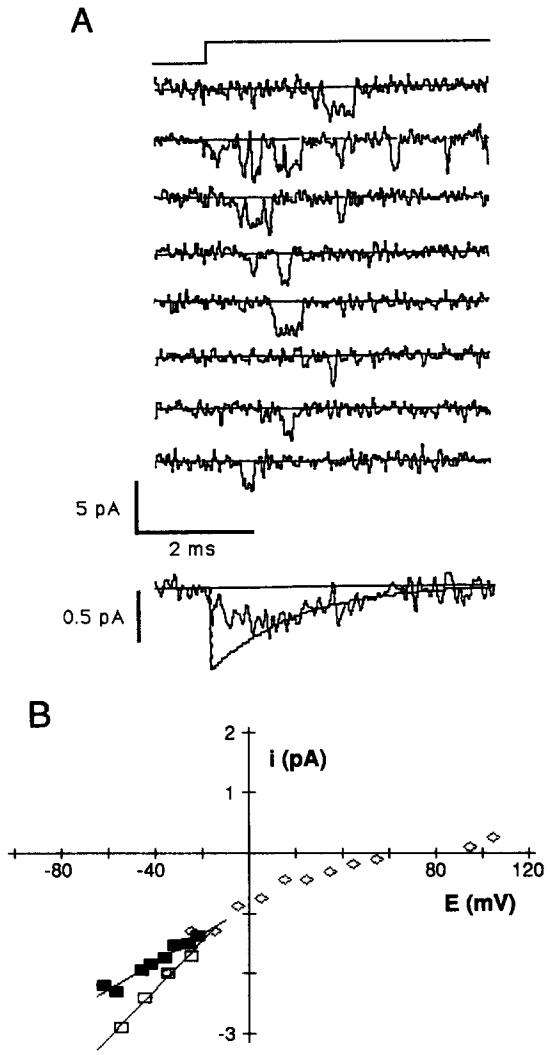

FIGURE 7. (*A*) Single-channel current records from an inside-out patch in 200 Na//200 K solutions. Selected nonconsecutive current traces are shown in response to 5-ms depolarizations to −65 mV after a 20-ms prepulse to −125 mV. Openings are downward from the baseline. The holding potential was −95 mV and the interval between pulses was 1 s. The average of 40 consecutive sweeps is shown at the bottom; it decays with a time constant of 1.2 ms. The filter was 10 kHz for the single channel current records and 5 kHz for the average current trace. (*B*) Single-channel current–voltage relations. (◇) Values of i from variance-mean analysis in 200 Na//200 K; (■ and □) direct measurement of single channel currents in 200 Na//200 K (same experiment as in *A*), and 400 Na//400 K, respectively. Single-channel current values are averages of 6–10 amplitudes measured from relatively long (>0.5 ms) openings with flat tops. Files: (◇) 8179a.n1a, (■) 5059c.sa, (□) 12029a.sia.

Single Channel Recordings

Fig. 7 *A* shows current traces displaying individual openings during depolarizations to −65 mV recorded in an inside-out patch in 200 Na//200 K, on the day after the dissection. The average current from 40 consecutive sweeps is plotted at the bottom. The single-channel current values from this patch (filled squares in Fig. 7 *B*) yield a

slope conductance of 23 pS in the voltage range of −60 to −20 mV. The same conductance is obtained from variance-mean analysis of macroscopic currents (*diamonds*) in a patch from a freshly dissected cell. In 400 Na//400 K the single-channel currents (*open squares*) showed a slope conductance of 40 pS in the range −55 to −25 mV.

Comparison of Currents on Day 1 and Day 2

No apparent differences were observed in the activation and inactivation of the currents recorded from freshly dissected cells (day 1) and those recorded from cells

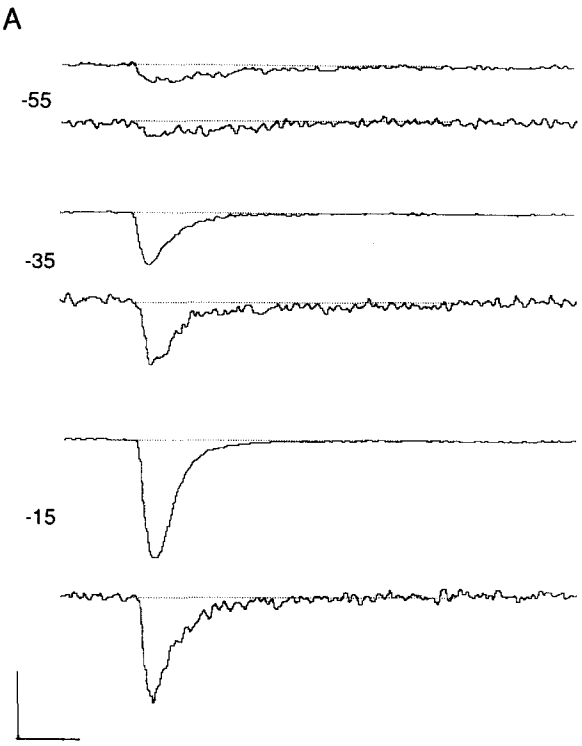

FIGURE 8. Comparison of currents on day 1 and day 2. (*A*) Each pair of traces compares the average macroscopic current (*upper*) from 6 consecutive sweeps recorded from a freshly dissected cell (File: 8159c.1a), with the average of 20 consecutive sweeps (*lower*) recorded from the same preparation on the day after the dissection (File: 8169a.1a). Currents were recorded in inside-out patches and were elicited by step depolarizations after a 20-ms hyperpolarizing prepulse to −120 mV from a holding potential of −90 mV. Filter, 5 kHz. For the top trace in each set the vertical scale bar corresponds to 100 pA (−35 and −15 mV) and 35 pA (−55 mV), and 5 pA for each of the bottom traces. Horizontal, 2 ms. (*B*) Normalized peak current-voltage relations for (□) day 1 and (◇) day 2 currents. The data are from the patches in *A*. The currents from each day were normalized to the current at −5 mV (−263 pA and −9 pA, respectively). The solid curve is a least-squares fit to Eq. 1 with parameters: E_a = +13 mV, z_a = 1.8, P_{Na}/P_K = 28, P_{Na} = 2.7 × 10^{-7} cm/s. (*C*) Voltage dependence of τ_h for (□) day 1 and (◇) day 2 currents. Same patches as in *A*. The symbols correspond to the time constants of the visually fitted single-exponential functions.

on the day after the dissection (day 2). Each pair of traces in Fig. 8 *A* compares the large currents (upper) recorded on day 1 with the smaller currents (lower) recorded from the same preparation (but a different cell) on day 2; the upper and lower traces correspond to the average of 6 and 20 consecutive sweeps, respectively. The normalized peak current-voltage relations from day 1 (*squares*) and day 2 (*diamonds*) are shown in Fig. 8 *B*. The solid curve is a least-squares fit of Eq. 1 (see figure legend for parameters). Fig. 8 *C* compares the voltage dependence of τ_h for day 1 (*squares*) and day 2 (*diamonds*) currents.

Why are the currents smaller on day 2? The reduction in current is not apparent as a gradual run down on day 1; the average ratios of the currents measured 6, 10, 11, 13, and 27 min apart in five patches were 1.00, 1.04, 0.90, 1.04, and 1.00, respectively. We speculate that an increase in intracellular Ca resulting from storage of the tissue in a physiological extracellular solution at 4°C might have led to smaller currents on day 2. In favor of this view is the result of one experiment in which the tissue was stored in "Ca-free" extracellular solution overnight at 4°C. Under these

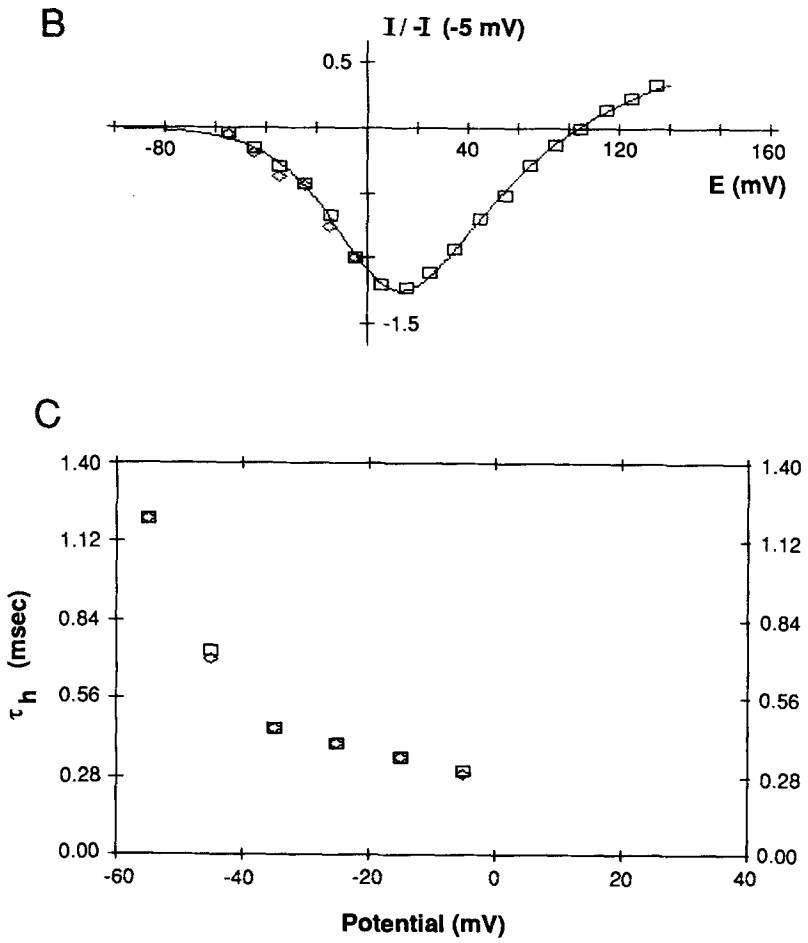

FIGURE 8. *(continued)*

conditions the current amplitudes that we measured on the following day were comparable to those on day 1. Further support of this hypothesis comes from patch-clamp experiments on squid giant axons, where exposure of the inside of a freshly dissected axon to sea water containing Ca for a few minutes leads to a reduction of the Na current density without affecting channel kinetics (Bezanilla, 1987).

TABLE III

Selectivity Ratios in Various Preparations

Preparation	P_{Na}/P_K	Reference
Squid axon*	11.5	Chandler and Meves (1965)
Frog node‡	11.6	Hille (1972)
Myxicola axon§	10.0	Ebert and Goldman (1976)
Frog skeletal muscle‖	20.8	Campbell (1976)

*Internally perfused axon with 300 mM K. The external solution was K-free artificial sea water (473 mM Na). P_{Na}/P_K calculated from reversal potential measurements.

‡Cut fiber preparation in 110 mM K. P_{Na}/P_K calculated from reversal potential differences with 110 mM external Na and K solutions.

§Internally perused axon with 200 mM K. The external solution was K-free artificial sea water (440 mM Na). P_{Na}/P_K calculated from reversal potential measurements.

‖Cut fiber preparation in 120 mM Cs. P_{Na}/P_K calculated from reversal potential differences with 110 mM external Na and K solutions.

Reversal Potentials

The selectivity ratios in Na channels from nerve and muscle cells have been found to be well defined for given sets of ionic conditions (Table III). We were surprised to find that in inside-out patches with equal concentrations of Na outside and K inside, the measured reversal potentials varied from patch to patch from a single electrocyte. No variation was found in repeated measurements on a single patch. In a patch from Sachs cell 12, reversal potential measurements made 16 min apart were both +75 mV; in cell 15, identical values of +51 mV were measured at the beginning of the experiment and 21 min later. Fig. 9 *A* shows the peak current-voltage relations from three patches in 200 Na//200 K. The reversal potentials were +51, +77, and +92 mV. Families of currents recorded in the vicinity of the reversal potential from these patches are shown in *B*. In 27 inside-out patches from 18 Sachs cells the range of

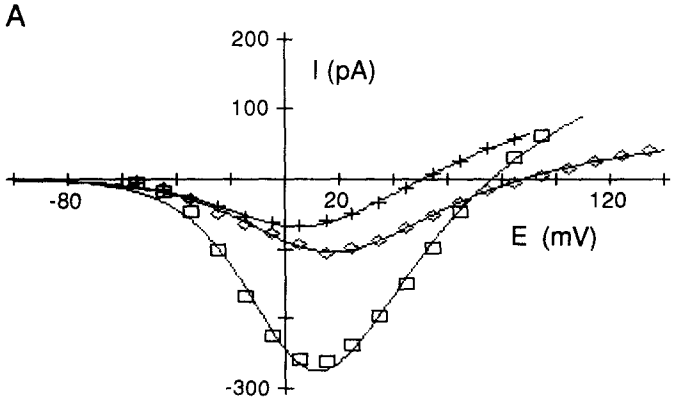

FIGURE 9. (*A*) Peak current–voltage relations of different patches in 200 Na//200 K solutions. The curves are least-squares fits of Eq. 1 with reversal potentials of 51 (+), 77 (□), and 87 mV (◇). (*B*) Families of currents in the vicinity of the reversal potential corresponding to the experiments in *A*. The dotted line in the top panel represents the baseline current level. Files: (+) 5169a.2a, (□) 8179b.1a, (◇) 10249a.1a.

measured reversal potentials was from +50 to +92 mV, with a mean of +75 ± 14 mV (SD; Table I). The mean reversal potential corresponds to a selectivity ratio P_{Na}/P_K of 20 with a range of 8 to 40. Reversal potential variation was also observed in 400 Na//400 K. However, under these conditions the currents reversed at a more positive

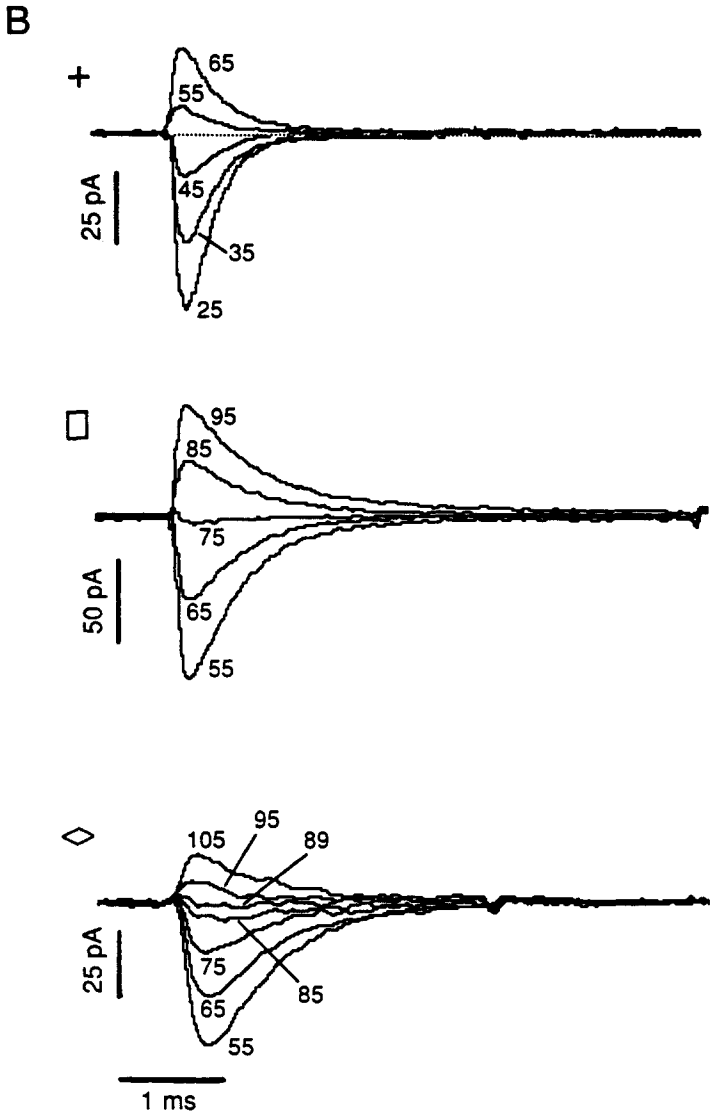

FIGURE 9. (*continued*)

potential on average and the range of variability was apparently lower: +86 ± 8 mV (mean ± SD) with a range of +75 to +96 mV in six patches from three cells. The range corresponds to P_{Na}/P_K of 20–46; it should be noted that the large P_{Na}/P_K of 41 found for trypsin-treated purified electrocyte Na channels in planar bilayers in 400

Na//400 K (Shenkel et al., 1989) is within the range of values observed here for the 400-mM solutions. A large variation in reversal potential values in inside-out patches from main organ electrocytes was also observed (Table II, *C* and *D*).

Controls for Errors in Reversal Potential Measurements

One source of error that could produce reversal potential variation from patch to patch would be drift in the electrode offset potential. Several tests ruled out such drifts. First, fluctuations in electrode offset potential difference with an open pipette in the bath were measured to be <1 mV. Second, the electrode potential difference was zeroed before each experiment and checked at the end. When present, offset potentials were at most 3 mV in those experiments analyzed for this paper.

Further tests of accurate voltage control involved comparison of the values of the reversal potential E_r and the inactivation midpoint potential E_h. The standard deviations of reversal potentials ranged from 14 to 19 mV compared with ≤ 5 mV for E_h (Table II, *A–D*), suggesting that their variations come from different sources. Comparison of the values for electrocytes 14 and 20 in Table II *A* shows a particularly large (40 mV) difference in E_r, but only a 3 mV difference in E_h. A correlation coefficient of $r = +1$ between E_h and E_r would be expected for correlated errors due to electrode drift, while a value near -1 would result from large series-resistance errors. Analysis of the E_h and E_r values in Table II *B* showed no correlation ($r = 0.16$; $P > 0.5$).

Additional tests of accurate voltage control of the patch, as well as of possible effects of ion accumulation or chloride permeability, involved experiments in symmetrical and asymmetrical NaCl solutions. Under these conditions E_r is expected to follow the Nernst equation for Na. Fig. 10 shows a family of currents recorded in symmetrical 200 Na along with peak current-voltage relations from three patches on the same cell. A reversal potential of +0.7 mV was obtained from a fit of Eq. 1 to the data indicated by the squares. The two other patches had reversal potentials of 0.8 and −0.2 mV.

A more sensitive test made use of asymmetric Na solutions on three patches from the same cell. First, the reversal potential was measured in 200 Na//20 Na + 327 sucrose. Under these conditions the calculated Nernst potential for Na is +60 mV at 24°C; the measured values were +60, +59, and +58 mV. (Fig. 11 *A*). Next, the bath side of the patch was perfused by moving the pipette tip into a steady stream of 200 K solution from a small diameter tube immersed in the bath, and reversal potentials of +66, +81, and +103 mV were measured (Fig. 11 *B*). Finally, moving the patch away from the stream resulted in the return of the reversal potential back to its previous value near +60 mV. The families of currents shown in Fig. 11 correspond to the data indicated by the diamonds in *A* and *B*. In three other patches from the same cell the measured reversal potentials in 200 Na//20 Na + 327 sucrose were in the range +58 to +62 mV. To test whether the perfusion with the 200 K solution was complete, the converse experiment was performed with 200 K in the bath and 200 Na in the perfusion tube. Reversal potentials of 0 mV were observed when the patch was moved into the 200 Na stream. The experiments in asymmetric Na solutions also served as a control for the possibility that the reversal potential variation arose from dilution of the pipette solution by the bath solution. Such dilution was unlikely since

slight positive pressure was always applied to the interior of the pipette resulting in the flow of solution away from the tip, and seal formation was almost instantaneous upon application of gentle suction.

We also considered the possibility that a transient K current might be present, which, if it had kinetics similar to the Na current, could influence the apparent reversal potential. Fig. 12 shows data from an experiment in which we looked for transient outward current with tetrodotoxin (TTX) in the pipette to block Na current. 11 patches were made from a single cell, 5 patches without TTX and 6 with 1 μM TTX present. Comparison of separate patches with and without TTX in the pipette was done because of the difficulty of perfusing the pipette with a TTX solution. In the absence of TTX the maximal Na currents from different patches were 40–115 pA

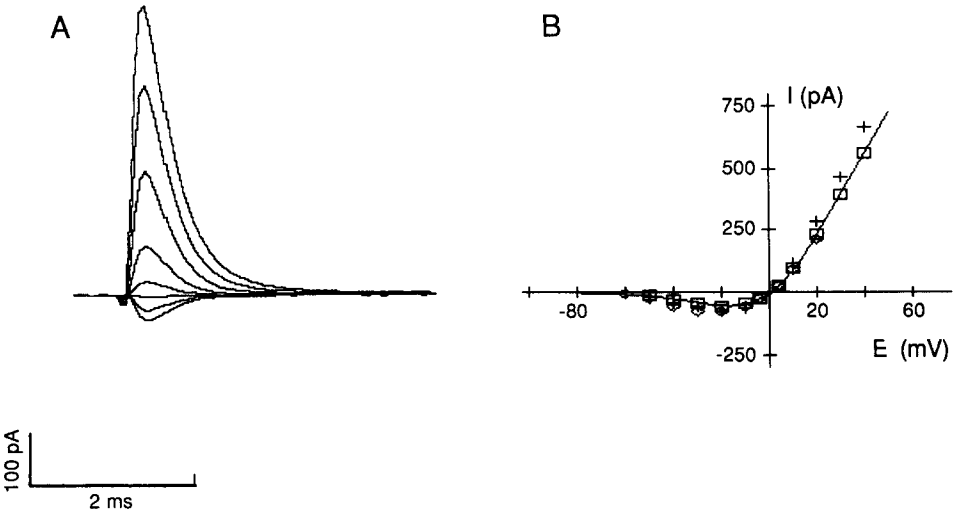

FIGURE 10. Mean currents and peak current–voltage relations recorded in 200 Na//200 Na solutions. (*A*) Decreasing inward currents (downward deflections) are shown in response to voltage steps of −10 and −4 mV; increasing outward currents correspond to steps in the range +4 to +40 mV. (*B*) Peak current-voltage relations in three patches from the same cell. The family of currents in *A* correspond to the □ symbols. Files: (□) 6089a.1a, (+) 6089a.2a, (◇) 6089a.3a.

and reversal potentials ranged from +47 to +81 mV. Fig. 12 *A* shows a family of currents in the vicinity of the reversal potential from one of the three patches before TTX. The next five patches were made in the presence of TTX; neither Na current nor transient outward current was observed. Fig. 12 *B* shows current traces from one of these patches. Na current was observed in the two ensuing patches in the absence of TTX (Fig. 12 *C*). For the final patch in this experiment TTX was used; again, no currents were seen (Fig. 12 *D*).

Finally, we wondered if the currents through the patch membrane could be large enough to influence the local ion concentration. Fig. 12 *E* shows an example of the total pipette current without P/4 leak subtraction. The trace shows fast and slow (time constant ~0.2 ms) capacitive components, mainly resulting from the stray capaci-

tance in the wall of the pipette. The fast component is inverted, resulting from slight overcompensation of "c-fast" on the patch-clamp amplifier. The large slow component arises from dielectric relaxation in the pipette glass ("bulk ac conductance," see Hamill et al., 1981); its full amplitude appears here because no "c-slow" compensation was used. The size of this component was smaller with pipettes having a thicker Sylgard® coating. The seal resistance for this patch, estimated from the current at the end of the depolarization, was 24 GΩ. The background current through the patch

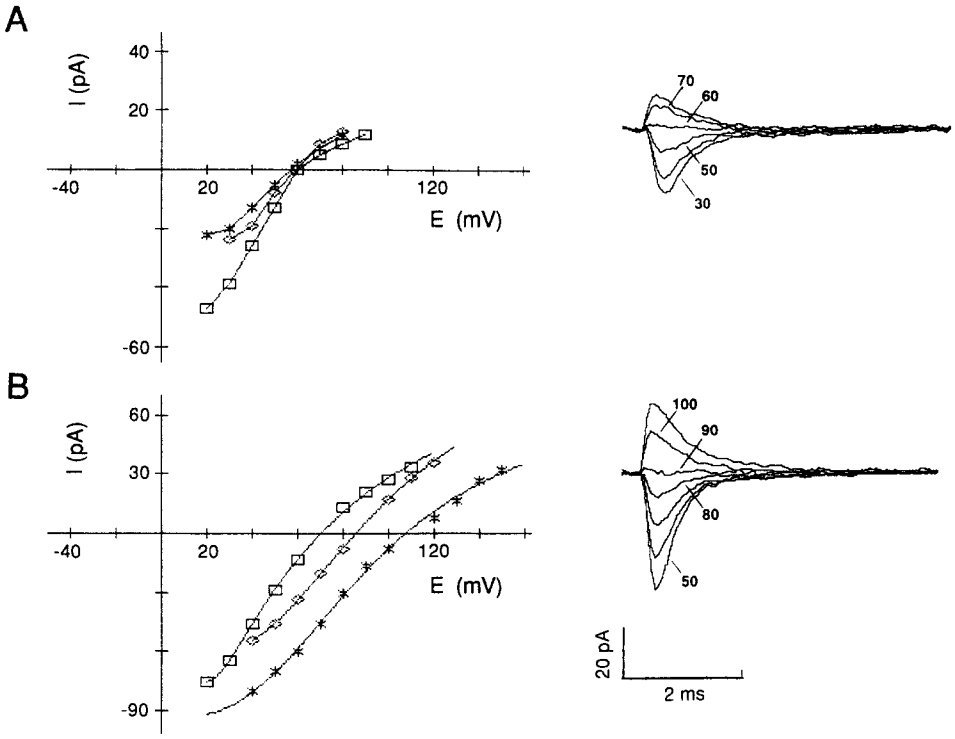

FIGURE 11. (*A*) Peak current-voltage relations in 200 Na//20 Na + 327 sucrose solutions. The three symbols correspond to three inside-out patches from the same cell. Files: (□) 7069c1.3b; (*) 7069c2.5b; (◇) 7069c3.7b. (*B*) Peak current-voltage relations after perfusion of the bath side of the patches in *A* with 200 K solution. The peak currents indicated by the asterisks were scaled up by a factor of two for convenience of comparison with the other curves. Files: (□) 7069p1.3b; (*) 7069p2.5b; (◇) 7069p3.7b. (*C* and *D*) Families of currents corresponding to the ◇ symbols in *A* and *B*, respectively.

membrane is seen to be < 10 pA. A steady cation flux corresponding to a current of this magnitude would result in a very small perturbation in cation concentration, on the order of 0.1 mM at the membrane surface, if we assume that the access resistance to the membrane is similar to the open-pipette resistance of 3 MΩ.

The reversal potential data from inside-out patches are summarized in Fig. 13. The symbols in *A* and *C* correspond to reversal potential measurements in 200 Na//200 K and 400 Na//400 K, respectively. Fig. 13 *B* summarizes the results with asymmetric

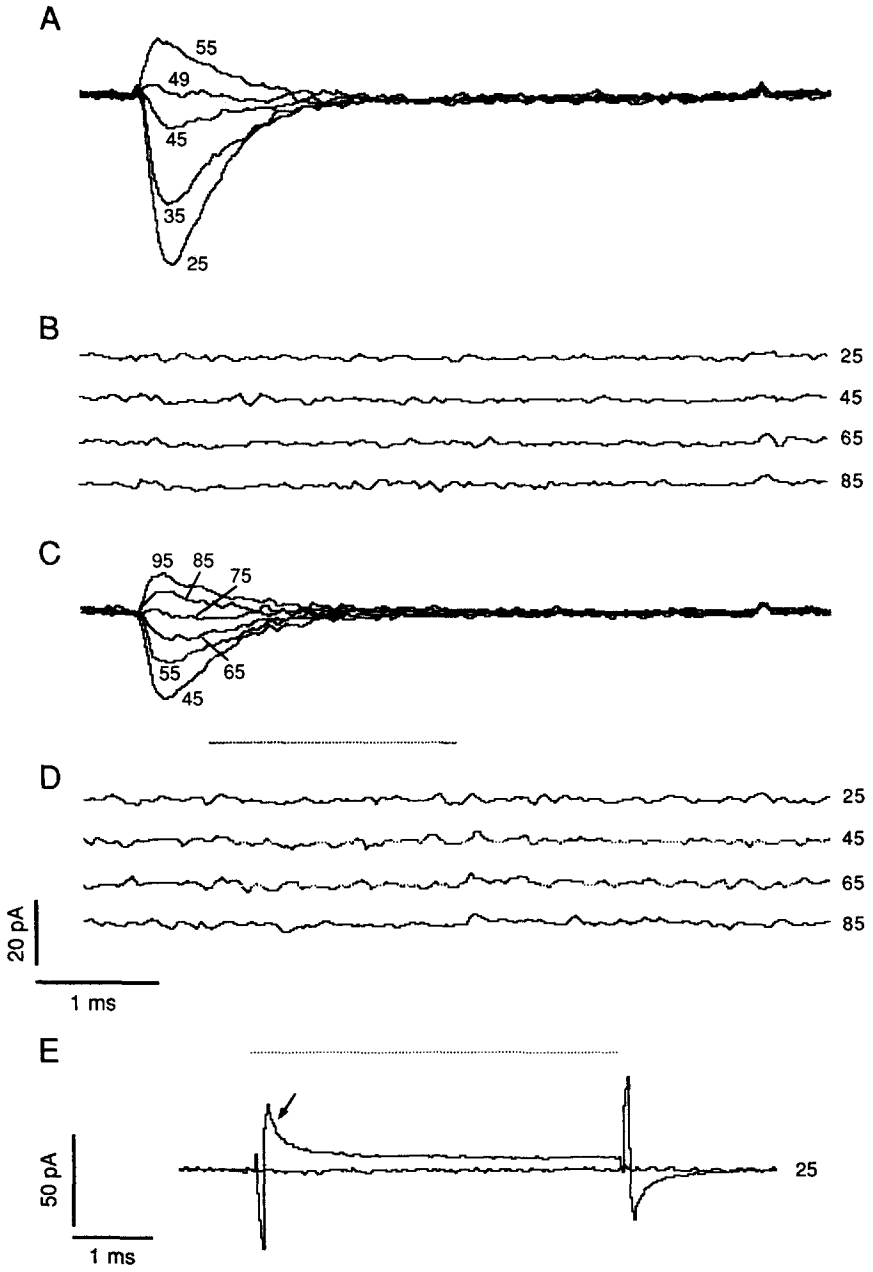

FIGURE 12. Absence of transient outward current. Recordings from inside-out patches from a single electrocyte in 200 Na//200 K (*A*, *C*) and with 1 μM TTX in the pipette solution (*B*, *D*). Step depolarizations to the voltages shown were applied at 0.5/s for durations (indicated by bar above records) of 5 ms (2 ms in *D*). The depolarizations followed 20-ms prepulses to −125 mV. The holding potential was −95 mV. (*A*) A family of currents in the vicinity of the reversal potential (+47 mV) in the absence of TTX. File: 01109a.1a. (*B*) Current traces in the presence of 1 μM TTX in the pipette. File: 01109a.2b. (*C*) A family of currents in the vicinity of the reversal potential (+75 mV) in the absence of TTX. File: 01109a.2c. (*D*) Current traces in the presence of 1 μM TTX. File: 01109a.1d. (*E*) Superimposed current traces during a step depolarization to +25 mV in the presence of 1 μM TTX without leak subtraction (*arrow*) and after P/4 subtraction. The steady current at the −90 mV holding potential was −3 pA; this was subtracted from the trace. Same patch as in *B*.

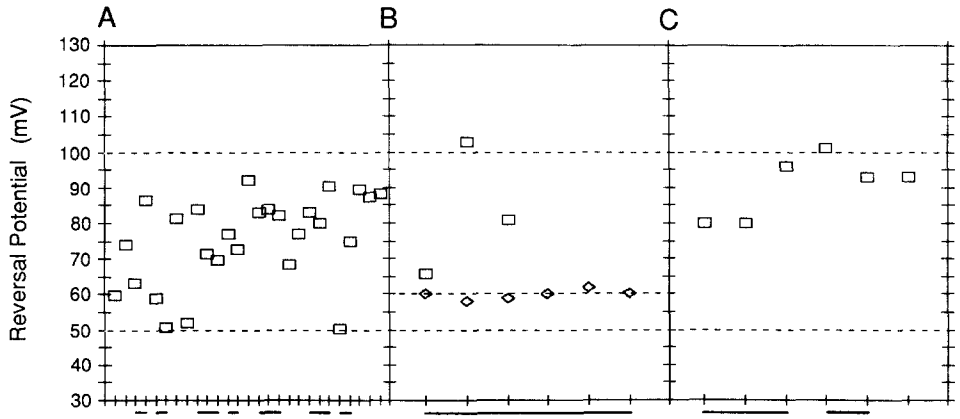

FIGURE 13. Summary of reversal potential measurements in Sachs organ electrocytes. (*A*) Reversal potentials in individual patches are plotted in chronological order for 27 experiments in 200 Na//200 K made over a 7-mo period. (*B*) Reversal potentials measured in asymmetric Na solutions (200 Na//20 Na + 327 sucrose) (◇), compared with reversal potentials from the same patch after perfusion with 200 K in the bath (□). The middle dashed line indicates the expected reversal potential of +60 mV for the asymmetric Na solutions. (*C*) Reversal potentials plotted in chronological order from experiments using 400 Na//400 K. Horizontal bars at the bottom indicate patches from the same cell.

Na solutions. The diamonds are reversal potentials obtained in 200 Na//20 Na + 327 sucrose; the corresponding reversal potentials after perfusion of the same patches with 200 K solution are shown as squares.

DISCUSSION

We have presented here an initial characterization of the currents through electric eel electrocyte Na channels, based on patch-clamp recordings of macroscopic and single-channel currents in electrocytes from the Sachs and main electric organs. Biochemical studies have used the main organ as the source of Na channel protein; the currents we have recorded in electrocytes from the main organ and organ of Sachs have very similar properties. The density of channels is quite high: the maximal patch currents in Sachs cells ranged from 20 to 300 pA (27 patches), and from variance-mean analysis the estimated number of channels in a patch was 70 to 1,350. Assuming a patch area of 10 μm^2, this corresponds to ~10–100 channels/μm^2, lower than the ~500/μm^2 estimated from toxin binding experiments (Levinson, 1975) in main organ, but consistent with the density of ~100/μm^2 we calculate from our values of P_0 and i and the peak current density of ~3 mA/μF (~30 pA/μm^2) observed by Nakamura et al. (1965) in electrocytes from the organ of Sachs. The peak currents we measure in main organ electrocytes were approximately twofold greater on average than those in Sachs cells, which probably reflects a higher channel density. It is interesting to note that overnight storage of tissue at 4°C reduced the number of active channels in a patch to ~1/100 of the number in freshly dissected cells. No evidence of run-down was seen in long patch recordings, however. Perhaps the decrease in channel density, which we speculate might be Ca dependent, arises

from removal of channels from the membrane, or from a cell regulatory process by which the channels are turned off but still reside in the membrane.

The general features of the Na channel currents observed here are similar to those reported by Nakamura et al. (1965) in their voltage-clamp analysis of relatively large areas of innervated membrane (0.02–0.07 cm^2). They observed rapidly activating inward currents that lasted 0.5–1 ms during maintained depolarizations at 22°C, and in physiological saline, reversed at +62 mV. A major difference between our recordings and the results of the voltage-clamp work has to do with K conductances. The electrocyte innervated membrane was reported to have a remarkably low resting membrane resistance of $\sim 5\ \Omega cm^2$ (Keynes and Martins-Ferreira, 1953; Nakamura et al., 1965), which arises mainly from an inward-rectifying K conductance (reviewed in Grundfest, 1966). In voltage-clamp experiments the membrane resistance is seen to increase with depolarization from rest (Nakamura et al., 1965), but the resistance increase is only about a factor of two, limited by what appears to be a substantial, K-selective leak conductance (G_L; Ruiz-Manresa and Grundfest, 1976). We did not observe inward rectifier currents, but this is not surprising since our extracellular solutions contained no potassium (Hagiwara et al., 1976). It is surprising, however, that a large leakage conductance is not reflected in our seal resistance values, which were similar to those reported by Pasquale et al. (1986) in their patch-clamp experiments on eel electrocytes. These values represent the parallel combination of seal leakage resistance and membrane resistance, and therefore can be taken only as a lower bound on the resistance of the patch membrane. From our values in Table I it can be concluded that the membrane resistance was always $> 3\ G\Omega$ in our patches; in one patch where the peak Na current was nearly 300 pA, the lower bound is 63 GΩ. On the other hand, a membrane leakage resistance of 10 Ωcm^2 translates to 100 MΩ in a 10-μm^2 patch. If we take into account the geometrical factor implied by a specific capacitance of $\sim 50\ \mu F/cm^2$ (Nakamura et al., 1965), the predicted patch resistance is still only 5 GΩ.

An explanation for this order-of-magnitude discrepancy in membrane resistances could be a leakage artifact in the early voltage-clamp experiments. In the voltage-clamp system an intact cell is sandwiched between plastic sheets, forcing current to flow through both the noninnervated and innervated membranes, while the innervated membrane potential is measured from an intracellular microelectrode (Nakamura et al., 1965). In this configuration, leakage current that passes around the outside of the cell appears as a current that reverses at the cell's resting potential. It is not immediately obvious as a leak because it does not reverse at zero membrane potential. There is no simple way to measure or control the conductance of this leak pathway. We suggest that this artifact might have contributed a substantial part, or possibly all, of the large leak conductance observed in the voltage-clamp results, and that the electrocyte membrane has a much lower leakage conductance than previously thought.

The fast inactivation properties of electrocyte Na channels appear generally similar to those of nerve and muscle channels (Hodgkin and Huxley, 1952; Goldman and Schauf, 1972; Campbell and Hille, 1976). The inactivation phase during maintained depolarizations was well fitted by a single exponential function. In a few patches the outward Na current decayed to a steady nonzero level during strong depolarizations.

An outward current resembling delayed K current activation was also observed in some patches. The decrease in the inactivation time constant in the voltage range of −65 to ~0 mV is similar to other Na channels. In our recordings the time constants were seen to gradually increase for depolarizations greater than +10 mV; this appears to be a unique property of the eel channel. The average midpoint voltage of the steady-state inactivation curve for the eel channel is ~14 mV more negative than in frog skeletal muscle and node (Campbell and Hille, 1976) and 45 mV more negative than in squid axon (Hodgkin and Huxley, 1952), but the steepness of the curves corresponds to an apparent valence of ~4 in each case.

No shifts in gating were observed for Na channels in membrane patches after excision. This was surprising, since patch excision in other cell types produces negative shifts of 10–50 mV in channel activation and inactivation properties (Fenwick et al., 1982; Cachelin et al., 1983; Fernandez et al., 1984).

Similar single-channel conductance values were obtained from direct measurement of channel currents and from fluctuation analysis, and these values are comparable to those observed in other Na channels (Hille, 1984). In inside-out patches with 200 Na//200 K solution the single-channel slope conductance was ~20 pS in the voltage range of −60 to −20 mV. This value is similar to the 16–17 pS (in 250 mM Na) reported by Rosenberg et al. (1984*b*) for purified eel channels in patch-clamped liposomes. With 400 Na//400 K, the slope conductance was 40 pS in the voltage range of −55 to −25 mV. This is close to the 44 pS conductance in symmetrical 400 Na of trypsin-treated, purified eel Na channels in planar bilayers (Shenkel et al., 1989). It should be noted that the symmetric Na solution and the absence of divalent cations in the bilayer experiments would both tend to increase the conductance.

A surprising finding is the large variation in the selectivity ratio P_{Na}/P_K among inside-out patches observed under identical conditions. Values of P_{Na}/P_K, obtained by fitting the GHK current equation to the peak current–voltage relations, ranged from 8 to 40 (27 inside-out patches from 18 cells) in the organ of Sachs, and from 11 to 55 (4 inside-out patches from 4 cells) in the main organ. Variation was also seen among patches on a single cell (Tables I and II). In referring to Table I there appears to be a correlation between the magnitude of I_{max} and the P_{Na}/P_K selectivity ratio where larger values of I_{max} correspond to higher P_{Na}/P_K. The P_{Na}/P_K values were averaged in groups of nine in which the first group corresponded to the nine lowest values of I_{max}, the second group to the next highest, and the third group the highest values of I_{max}. The resulting average P_{Na}/P_K selectivity ratios from the three groups were (mean ± SEM): 18.7 ± 2.7, 21.3 ± 4.0, and 28.0 ± 2, respectively, with the corresponding average I_{max} values of 46, 102, and 248 pA. The existence of such a correlation is interesting, although the direction of the trend is puzzling: most artifacts, such as errors due to series resistance or diffusion of ions, would tend to reduce the apparent selectivity at higher current levels, not increase it. Interestingly, under conditions of higher ionic strength, average-size currents were associated with a relatively high P_{Na}/P_K. In the four patches with 400 Na//400 K in which I_{max} was measured, the average values of I_{max} and P_{Na}/P_K were 113 pA and 34 ± 5.5 (mean ± SEM).

The observed selectivity ratios tend to be higher than those reported in other preparations (Table III); it should be noted that a ratio of ~40 was also observed

with trypsin-treated eel channels in bilayers (Shenkel et al., 1989). It is not known whether unmodified, purified, reconstituted Na channels display such P_{Na}/P_K variability as direct reversal potential measurements have not been made. Rosenberg et al. (1984*b*) and Correa et al. (1990) both studied the properties of unmodified, purified eel Na channels in patch-clamped liposomes, but they were unable to measure single-channel currents on both sides of the reversal potential.

Several controls involving Na gradients, steady-state inactivation curves, and TTX have, in our opinion, ruled out sources of error due to electrode drift, voltage non-uniformity across the patch, ion accumulation effects, and the presence of contaminating K currents in our experiments. If the observed variation were an artifact, the most likely explanation would be the formation of a vesicle at the pipette tip causing a distortion of the inside-out patch recordings, and a change in the voltage applied to the Na channels. It appears to us, however, that the resulting change in potential or ionic concentrations at the membrane would also be detected as shifts in the inactivation curve or as changes in the reversal potential in asymmetric Na solutions. Neither of these effects was observed, leading us to believe that there are Na channels with differing selectivities in the electrocytes.

Our reversal potential measurements were made from populations of a few hundred channels, many fewer than the 10^5 to 10^8 channels found in the cellular preparations listed in Table III. In those preparations the number of channels is so large that mixtures of channels having different reversal potentials could exist in these preparations without any apparent effect on the macroscopic currents. Actually, our populations of several hundred channels should also have provided considerable averaging of channel properties. Suppose for example that there were two types of Na channels with similar conductance and equal probabilities of being present but with reversal potentials that differed by 100 mV. In a patch containing $N = 100$ channels the standard deviation of the reversal potential would be only 5 mV. The much larger scatter in reversal potentials that we observed suggests that channels with differing selectivities are not uniformly distributed, but are clustered in such a way that a patch membrane contains predominantly one type or another.

One situation in which selectivity variations among individual channels would be apparent is in bilayer studies of single BTX- or veratridine-activated Na channels, where the long channel-open times allow channel currents to be measured accurately on both sides of the reversal potential. However, in considering these results it should be kept in mind that the selectivity properties of BTX- or veratridine-activated channels are different from those of unmodified Na channels (Khodorov, 1985). P_{Na}/P_K has been determined from reversal potential measurements with reversed gradients of Na and K (Krueger et al., 1983; Moczydlowski et al., 1984; Garber, 1988) to be ~ 15, while under near-physiological ionic conditions the ratio is observed to be near 5.0 (Green et al., 1987; Recio-Pinto et al., 1987; Garber, 1988; Shenkel et al., 1989). These latter studies report standard deviations in reversal potentials of < 1.0, 2.4, 5, and 6 mV, respectively, which could, at least in part, be due to measurement error. On the other hand, results from purified, veratridine-activated eel channels by Duch et al. (1989) show reversal potentials in the range of -33 to -62 mV for a reversed gradient and $+40$ to $+52$ for a normal gradient of 455 mM Na and K; the scatter might have resulted from measurement errors, but it is

very large compared with the estimated electrode offset errors (<2 mV) and suggests that variability is present.

If there are multiple Na channel types in eel electrocytes, they could represent different gene products or different states of modification of a single species of Na channel protein. It is not known whether there are multiple Na channel genes in *Electrophorus* (as there are, for example in rat brain and muscle: Noda et al., 1986; Kayano et al., 1988; Auld et al., 1988; Trimmer et al., 1989; Kallen et al., 1989). There is no evidence from biochemical studies, however, for heterogeneity in the channel protein. On the other hand, it is known that the channel is heavily glycosylated (Miller et al., 1983) and is covalently modified in vivo by acylation (Thornhill and Levinson, 1986) and phosphorylation (Emerick and Agnew, 1989). It is tempting, therefore, to imagine that either the carbohydrate on the extracellular face of the channel, representing an estimated 200 negative charges, or phosphate groups attached on the intracellular face, could affect the selectivity of the channel by altering the electrostatic environment near the structures that determine the channel selectivity. Consistent with this kind of mechanism is the observation of Cahalan and Begenisich (1976) of higher selectivity ratios at higher ionic strengths; our data show a similar trend. However, it should be noted that in the absence of Ca the permeability ratio is concentration independent in neurotoxin-modified rat skeletal muscle Na channels in planar lipid bilayers under biionic conditions (Garber, 1988).

We thank F. Bezanilla, in whose laboratory preliminary recordings from main organ electrocytes were made. We also thank W. S. Agnew, E. Moczydlowski, and S. M. Sine for helpful comments on the manuscript, and S. M. Crean for assistance with eel care.

This work was supported by grants NS-21501 and NS-17928 from the National Institutes of Health.

Original version received 31 January 1990 and accepted version received 15 November 1990.

REFERENCES

Affolter, H., and F. J. Sigworth. 1988. High performance Modula-2 programs for data acquisition and analysis of single channel events. *Biophysical Journal.* 53:154 (Abstr.).

Agnew, W. S., S. R. Levinson, J. S. Brabson, and M. A. Raftery. 1978. Purification of the tetrodotoxin-binding component associated with the voltage-sensitive sodium channel from *Electrophorus electricus* electroplax membranes. *Proceedings of the National Academy of Sciences, USA.* 75:2606–2610.

Auld, J. V., A. L. Goldin, D. S. Krafte, J. Marshall, and J. M. Dunn. 1988. A rat brain Na channel α subunit with novel gating properties. *Neuron.* 1:449–461.

Bennett, M. V. L. 1971. Electric organs. *In* Fish Physiology. W. S. Hoar and D. J. Randall, editors. Academic Press, New York. 347–491.

Bezanilla, F. 1987. Single sodium channels from the squid giant axon. *Biophysical Journal.* 52:1087–1090.

Bezanilla, F., and C. M. Armstrong. 1977. Inactivation of the sodium channel. I. Sodium current experiments. *Journal of General Physiology.* 70:549–566.

Cachelin, A. B., J. E. De Peyer, S. Kokubun, and H. Reuter. 1983. Sodium channels in cultured cardiac cells. *Journal of Physiology.* 340:389–401.

Cahalan, M. D., and T. Begenisich. 1976. Sodium channel selectivity: dependence on internal permeant ion concentration. *Journal of General Physiology.* 68:111–125.

Campbell, D. T. 1976. Ionic selectivity of the sodium channel of frog skeletal muscle. *Journal of General Physiology.* 67:295–307.

Campbell, D. T., and B. Hille. 1976. Kinetic and pharmacological properties of the sodium channel of frog skeletal muscle. *Journal of General Physiology.* 67:309–323.

Chandler, W. K., and H. Meves. 1965. Voltage clamp experiments on internally perfused giant axons. *Journal of Physiology.* 180:788–820.

Correa, A. M., F. Bezanilla, and W. S. Agnew. 1990. Voltage activation of purified eel sodium channels reconstituted into artificial liposomes. *Biochemistry.* 29:6230–6240.

Duch, D. S., E. Recio-Pinto, C. Frenkel, S. R. Levinson, and B. W. Urban. 1989. Veratridine modification of the purified sodium channel α-polypeptide from eel electroplax. *Journal of General Physiology.* 94:813–831.

Ebert, G. A., and L. Goldman. 1976. The permeability of the Sodium channel in *Myxicola* to the alkali cations. *Journal of General Physiology.* 68:327–340.

Emerick, M. C., and W. S. Agnew. 1989. Identification of phosphorylation sites for cyclic AMP-dependent protein kinase on the voltage-dependent sodium channel from *Electrophorus electricus*. *Biochemistry.* 28:8367–8380.

Fenwick, E., A. Marty, and E. Neher. 1982. Sodium and calcium channels in bovine chromaffin cells. *Journal of Physiology.* 331:599–635.

Fernandez, J. M., A. P. Fox, and S. Krasne. 1984. Membrane patches and whole cell membranes: a comparison of electrical properties in rat clonal pituitary (GH_3) cells. *Journal of Physiology.* 356:565–585.

Garber, S. S. 1988. Symmetry and asymmetry of permeation through toxin-modified Na channels. *Biophysical Journal.* 54:767–776.

Goldman, D. E. 1943. Potential, impedance, and rectification in membranes. *Journal of General Physiology.* 27:37–60.

Goldman, L., and C. L. Schauf. 1972. Inactivation of the sodium current in *Myxicola* giant axons. Evidence for coupling to the activation process. *Journal of General Physiology.* 59:361–384.

Green, W. N., L. B. Weiss, and O. S. Andersen. 1987. Batrachotoxin-modified sodium channels in planar lipid bilayers: ion permeation and block. *Journal of General Physiology.* 89:841–872.

Grundfest, H. 1966. Comparative electrobiology of excitable membranes. *In* Advances in Comparative Physiology and Biochemistry. O. E. Lowenstein, editor. Academic Press, New York. 1–116.

Hagiwara, S., S. Miyazaki, and N. P. Rosenthal. 1976. Potassium current and the effect of cesium on this current during anomalous rectification of the egg cell membrane of a starfish. *Journal of General Physiology.* 67:621–638.

Hamill, O. P., A. Marty, E. Neher, B. Sakmann, and F. J. Sigworth. 1981. Improved patch-clamp techniques for high resolution current recording from cells and cell-free membrane patches. *Pflügers Archiv.* 391:85–100.

Hille, B. 1972. The permeability of the sodium channel to metal cations in myelinated nerve. *Journal of General Physiology.* 59:637–658.

Hille, B. 1984. Ionic Channels of Excitable Membranes. Sinauer Associates, Inc., Sunderland, MA. 426 pp.

Hodgkin, A. L., and A. F. Huxley. 1952. The dual effect of membrane potential on sodium conductance in the giant axon of *Loligo*. *Journal of Physiology.* 116:497–506.

Hodgkin, A. L., and B. Katz. 1949. The effect of sodium ions on the electrical activity of the giant axon of the squid. *Journal of Physiology.* 108:37–77.

Kallen, R. G., Z. Sheng, L. Q. Chen, K. Fischbeck, and R. L. Barchi. 1989. Characterization of a full-length cDNA for a sodium channel differentially expressed in denervated rat skeletal muscle. *Society for Neuroscience Abstracts.* 15:197.

Kayano, T., M. Noda, V. Flockerzi, H. Takahashi, and S. Numa. 1988. Primary structure of rat brain sodium channel III deduced from the cDNA sequence. *Federation of European Biochemical Societies.* 228:187–194.

Keynes, R. D., and H. Martins-Ferreira. 1953. Membrane potentials in the electroplates of the electric eel. *Journal of Physiology.* 119:315–351.

Khodorov, B. I. 1985. Batrachotoxin as a tool to study voltage-sensitive sodium channels of excitable membranes. *Progress in Biophysics and Molecular Biology.* 45:57–148.

Krueger, B. K., J. F. Jennings, III, and R. J. French. 1983. Single sodium channels from rat brain incorporated into planar lipid bilayer membranes. *Nature.* 303:172–175.

Lester, H. A. 1978. Analysis of sodium and potassium redistribution during sustained permeability increases at the innervated face of *Electrophorus* electroplaques. *Journal of General Physiology.* 72:847–862.

Levinson, S. R. 1975. Studies on Excitable Membranes. Ph.D. Dissertation. University of Cambridge, Cambridge, England. 199 pp.

Luft, J. H. 1957. The histology and cytology of the electric organ of the electric eel (*Electrophorus electricus* L.). *Journal of Morphology.* 100:113–140.

Miller, J. A., W. S. Agnew, and S. R. Levinson. 1983. Principal glycopeptide of the tetrodotoxin/saxitoxin binding protein from *Electrophorus electricus:* isolation and partial chemical and physical characterization. *Biochemistry.* 22:462–470.

Moczydlowski, E., S. S. Garber, and C. Miller. 1984. Batrachotoxin-activated Na channels in planar lipid bilayers: competition of tetrodotoxin block by Na. *Journal of General Physiology.* 84:665–686.

Nakamura, Y., S. Nakajima, and H. Grundfest. 1965. Analysis of spike electrogenesis and depolarizing K inactivation in electroplaques of *Electrophorus electricus,* L. *Journal of Physiology.* 49:321–349.

Noda, M., T. Ikeda, T. Kayano, H. Suzuki, H. Takeshima, et al. 1986. Existence of distinct sodium channel messenger RNAs in rat brain. *Nature.* 320:188–192.

Noda, M., S. Shimizu, T. Tanabe, T. Takai, T. Kayano, et al. 1984. Primary structure of *Electrophorus electricus* sodium channel deduced from cDNA sequence. *Nature.* 312:121–127.

Pasquale, E. B., J. B. Udgaonkar, and G. P. Hess. 1986. Single channel current recordings of acetylcholine receptors in electroplax isolated from *Electrophorus electricus* main and Sachs electric organ. *Journal of Membrane Biology.* 93:195–204.

Recio-Pinto, E., D. S. Duch, S. R. Levinson, and B. W. Urban. 1987. Purified and unpurified sodium channels from eel electroplax in planar lipid bilayers. *Journal of General Physiology.* 90:375–395.

Rosenberg, R. L., S. A. Tomiko, and W. S. Agnew. 1984*a*. Reconstitution of neurotoxin modulated ion transport by the voltage-regulated sodium channel isolated from the electroplax of *Electrophorus electricus. Proceedings of the National Academy of Sciences, USA.* 81:1239–1243.

Rosenberg, R. L., S. A. Tomiko, and W. S. Agnew. 1984*b*. Single channel properties of the reconstituted voltage-regulated sodium channel isolated from the electroplax of *Electrophorus electricus. Proceedings of the National Academy of Sciences, USA.* 81:5594–5598.

Ruiz-Manresa, F., and H. Grundfest. 1976. Temperature dependence of the four ionic processes of spike electrogenesis in eel electroplaques. *Proceedings of the National Academy of Sciences, USA.* 73:3554–3557.

Shenkel, S. 1989. Patch-clamp characterization of native Na channels from electrocytes of the electric eel *Electrophorus electricus. Society for Neuroscience Abstracts.* 15:537.

Shenkel, S., E. C. Cooper, W. James, W. S. Agnew, and F. J. Sigworth. 1989. Purified, modified eel sodium channels are active in planar bilayers in the absence of activating neurotoxins. *Proceedings of the National Academy of Sciences, USA.* 86:9592–9596.

Sigworth, F. J. 1980. The variance of sodium current fluctuations at the node of Ranvier. *Journal of Physiology.* 307:97–129.

Thornhill, W. B., and S. R. Levinson. 1986. Biosynthesis of electroplax sodium channels. *Annals of the New York Academy of Sciences.* 479:356–363.

Trimmer, J. S., S. S. Cooperman, S. A. Tomiko, J. Zhou, S. M. Crean, et al. 1989. Primary structure and functional expression of a mammalian skeletal muscle sodium channel. *Neuron.* 3:33–49.